Journal of Nuclear Materials 159 (1988) 101–113
North-Holland, Amsterdam

MEASUREMENT OF IRRADIATION CREEP OF ZIRCONIUM ALLOYS USING STRESS RELAXATION

A.R. CAUSEY, F.J. BUTCHER and S.A. DONOHUE

Metallurgical Engineering Branch, Chalk River Nuclear Laboratories, Chalk River, Ontario, K0J 1J0 Canada

Bent-beam stress relaxation tests provide a simple means of assessing the in-reactor creep behaviour of zirconium alloys with different prior thermo-mechanical treatments. By assuming that stress relaxation is equivalent to creep under decreasing stress, the irradiation-induced creep rate can be derived from tests in which small elastically constrained beams are exposed to fast neutron irradiation. In-reactor creep rates for stresses below about 150 MPa have been observed to depend linearly on applied stress, namely $\dot{\epsilon} = C\sigma\phi$, hence the stress relaxation behaviour can be described by the relation $\sigma/\sigma_0 = D\exp(-CE\phi t)$ where σ/σ_0 is the ratio of the unrelaxed stress (derived from the change in curvature of the unconstrained beam) to the initial stress to bend the beam to the shape of the jig, D describes an initial rapid stress drop, C is a material constant, E is Young's modulus, ϕ is fast neutron flux and t is time. We review stress relaxation test results that have been used to characterize the effects of operating parameters (such as temperature, fast neutron flux and fluence) and microstructural properties (such as anisotropy, dislocation structure, grain shape, thermo-mechanical treatments and alloy content) on the in-reactor creep behaviour of zirconium alloys. Correlations between stress relaxation and creep results are also presented with support the use of the relaxation test for gathering in-reactor creep information. Strain recovery in in-reactor and out-reactor annealing experiments suggest that in addition to anelastic strain, a significant part of the in-reactor relaxation strain is due to irradiation damage-related creep.

1. Introduction

The first convincing experimental evidence of the enhancement of creep in zirconium alloys by neutron irradiation was provided by Fidleris [1] using uniaxial tests at Chalk River Nuclear Laboratories in 1962. Subsequent experiments on large Zircaloy-2 and Zr–2.5Nb loop tubes in the National Reactor Universal test reactor (NRU) showed that transverse strain rates increased significantly during in-reactor service compared with rates measured in laboratory tests [2]. Unexpected elongations of power reactor pressure tubes have also been measured [3,4]. These dimensional changes have been attributed to a combination of stress-induced creep and stress-independent irradiation growth strains. Considerable effort has been expended in trying to measure and understand the effect of fast neutron flux, temperature, stress, and microstructure of zirconium alloys on the creep and growth phenomena. In-reactor creep experiments using uniaxial and tube specimens are difficult and expensive, particularly if the strain measurements are made in-situ.

Enhanced stress relaxation in-reactor has been reported for many metals and alloys [5–9]. Testing techniques such as those used by Hesketh [8] and Kreyns and Burkart [9], in which many small beam specimens were tested together under nearly identical conditions in limited reactor space, demonstrate the principal advantage of the stress relaxation test. A further advantage of the bent beam stress relaxation test is that irradiation growth does not affect the curvature change and thus all strains are a measure of creep alone. In this paper we review the stress relaxation tests carried out at CRNL over the past 20 years and their contribution to the understanding of the in-reactor creep behaviour of zirconium alloys. Experimental support for the equivalence between stress relaxation and creep is presented along with post-irradiation and in-situ annealing results which attempt to elucidate the inelastic and anelastic strain contributions during stress relaxation.

2. Experimental details

2.1. Test details

The experimental procedure used at CRNL is similar to that first reported by Kreyns and Burkart [9] in which several small beams were irradiated while held in

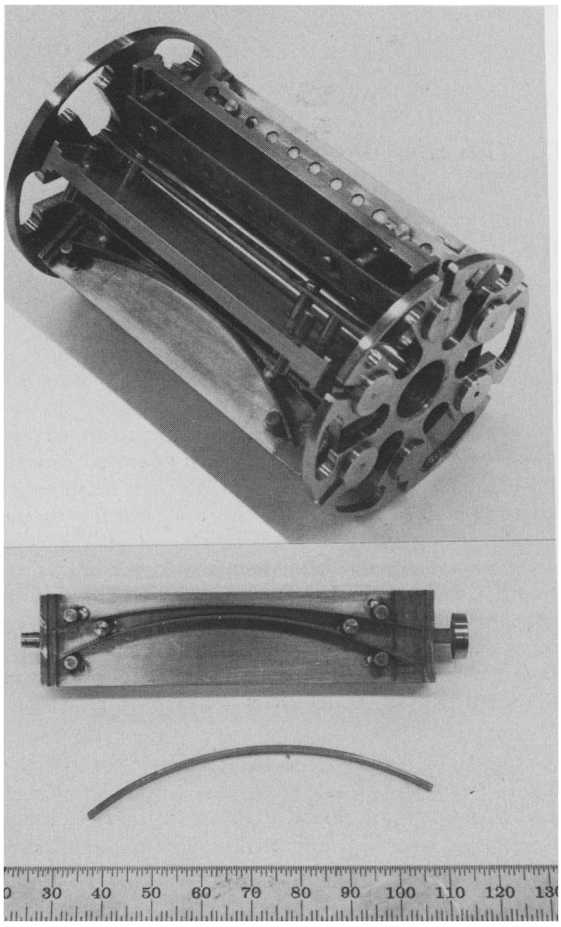

Fig. 1. Bent-beam stress relaxation specimens, four-point bending jig which holds specimens on both sides and spool which supports holders in the reactor insert.

jigs machined to radii which gave maximum outer fibre stresses ranging from 100 to 250 MPa. Our initial experiments [10] also stacked several specimens together but difficulties with crevice corrosion between the specimens from LiOH in the loop coolant water led to the use of four-point loading jigs shown in fig. 1. Specimens with the dimensions shown in figs. 2(a) and (b) were cut from sheet, pressure tube and calandria tube test materials. The jigs were mounted on spools, also shown in fig. 1, which were suspended in the reactor loop coolant at temperatures in the ranges of 530–570 K or 320–340 K. Fast neutron fluxes from 1.5 to 6.5×10^{17} n/m^2 s ($E > 1$ MeV) were obtained from fuel rods surrounding the loop pressure containment tubes.

Periodically, the specimens were removed from the reactor and their unconstrained radii of curvature measured from shadow prints obtained by placing the specimens on light-sensitive paper and exposing it to ultraviolet light. The unrelaxed stress ratio was determined from the equation

$$\sigma/\sigma_0 = (1/R_t - 1/R_h)/(1/R_0 - 1/R_h), \quad (1)$$

where σ and σ_0 are the stresses at time t and at time $t = 0$, and R_t and R_0 are the radii of the unconstrained specimen at the same times, while R_h is the radius of the holder.

Stress relaxation can be considered equivalent to creep under decreasing stress with the elastic strain converted to inelastic strain. The total strain, ϵ_0, has elastic, ϵ_e, and inelastic, ϵ_i, components,

$$\epsilon_p = \epsilon_e + \epsilon_i. \quad (2)$$

If the total strain is held constant, with time

$$\dot{\epsilon}_e = -\dot{\epsilon}_i. \quad (3)$$

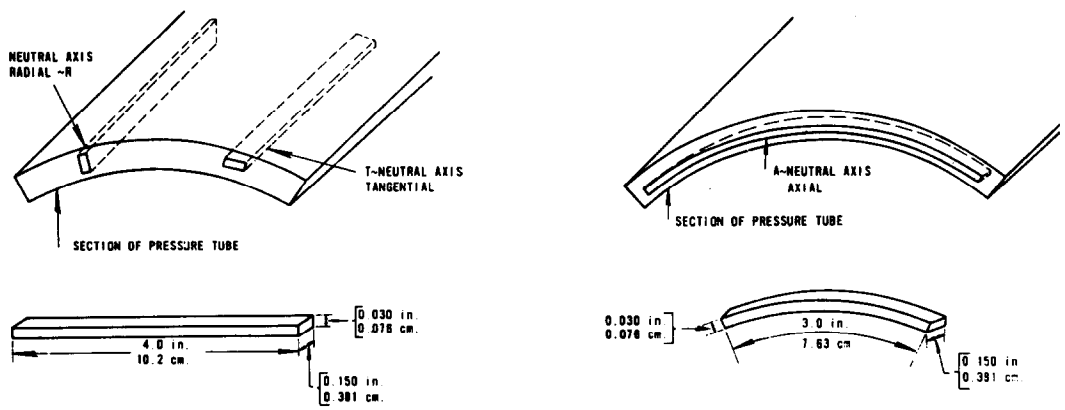

Fig. 2. Orientation and dimensions of stress relaxation beams taken from (a) longitudinal and (b) transverse directions of pressure tube.

In-reactor creep has been found to be governed by the law [2]

$$\dot{\epsilon}_i = C\phi\sigma, \tag{4}$$

where C is a temperature- and material-dependent constant, ϕ is the fast neutron flux and σ is the stress. By differentiating Hooke's law we have

$$\dot{\epsilon}_e = \dot{\sigma}/E, \tag{5}$$

where E is Young's modulus. Substituting eqs. (4) and (5) in eq. (3) and integrating we get the expression

$$\sigma/\sigma_0 = D\exp(-CE\phi t), \tag{6}$$

where σ and σ_0 are the stresses at time t and at time $t = 0$, D is an integration constant, and $K = CE\phi$ is the relaxation rate constant. Eq. (6) expresses the in-reactor relaxation behaviour in two stages: an initial rapid drop which includes thermal relaxation and transients, and a steady slower decrease in stress with time which depends on the irradiation conditions and material. The creep rate is obtained from the relaxation rate constant by

$$\dot{\epsilon}_i = (K/E)\sigma. \tag{7}$$

2.2. Data analysis

Typical stress relaxation results for specimens cut from the longitudinal direction of a cold-worked Zircaloy-2 pressure tube tested in the laboratory in an autoclave at 570 K and in-reactor at about 570 K in a flux of 1.8×10^{17} n/m^2 s are shown in fig. 3 [10]. The plot of ln σ/σ_0 as a function of time gives the initial drop, D, which is about the same for both in-reactor and out-reactor specimens. For the out-reactor test the rate of change of ln σ/σ_0 continuously decreases with time according to the approximate relation ln $\sigma/\sigma_0 \propto t^{1/3}$ so that after about 2000 h the relaxation rate has become negligibly small. The in-reactor relaxation continues at a steady rate which gives the relaxation rate constant K. The initial stresses of the specimens in this figure (and others in the same paper [10]) ranged from 100 to 250 MPa, with no apparent effect on the stress ratio, which is consistent with the linear stress dependence in the creep law in eq. (4) and is necessary for the use of bent beams in which the stress is proportional to the distance from the neutral axis. The out-reactor curve shown in fig. 3, where the stress dependence of the strain rate is greater than unity, is analytically indeterminate.

A correlation of creep rates derived from stress relaxation with constant-stress uniaxial creep tests on the same materials is shown in fig. 4 in which the strain rate is plotted as a function of stress [11]. There is good continuity in the curve from the creep rates at stresses below 100 MPa derived from stresses relaxation to the

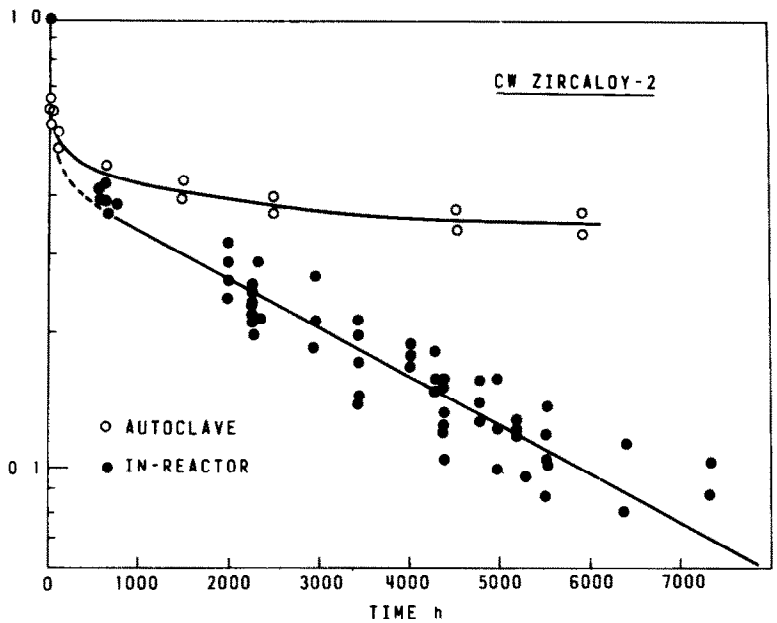

Fig. 3. Typical bent-beam stress relaxation data for longitudinal specimens of cold-worked Zircaloy-2 in-reactor in a fast neutron flux of 2×10^{17} n/m^2 s ($E > 1$ MeV) in water at 570 K and in an autoclave at 570 K [10].

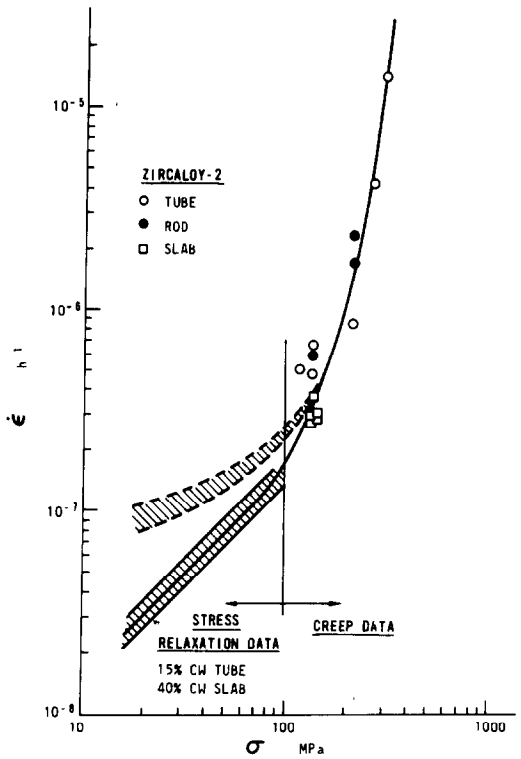

Fig. 4. In-reactor creep rate as a function of stress for Zircaloy-2 in a fast neutron flux of 1×10^{17} n/m^2 s ($E>1$ MeV) at 570 K. The band between the dashed lines represents the creep rate with an irradiation growth component added [11].

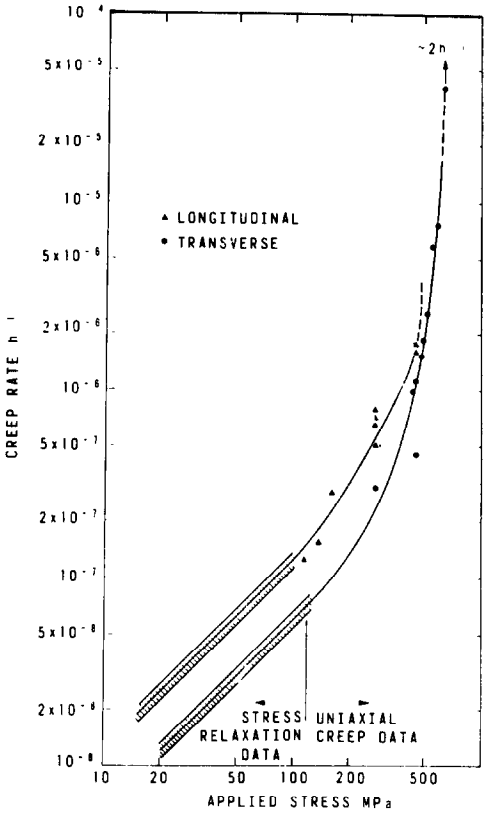

Fig. 5. Stress dependence of in-reactor creep rate of cold-worked Zr–2.5Nb pressure tube in a fast neutron flux of 1×10^{17} n/m^2 s ($E>1$ MeV) at 570 K [13].

strain rates in tests at 138 MPa and above obtained from continuously monitored creep machines [12]. The difficulties in measuring strain rates below 10^{-7} h^{-1} with creep machines are also complicated by strain contributions from irradiation growth, as illustrated by the dashed lines in fig. 4. In the bent-beam stress relaxation test, changes in curvature of the beams are wholy from creep strain and are not affected by irradiation growth strains. Similar trend curves from stress-relaxation-derived creep rates at low stress to uniaxial strain rates from tensile creep tests at stress above 100 MPa have been constructed for cold-worked Zr–2.5Nb, fig. 5 (without the correction for the growth component) [13].

3. Results and discussion

The in-reactor stress relaxation, and by inference and correlation, creep of zirconium alloys, is affected to some degree by many variables, both operational and metallurgical, including temperature, fast neutron flux, fluence, alloy content, cold work (dislocation structure), working direction (anisotropy) and grain size.

3.1. Temperature, flux and fluence

The temperature and flux dependence of the in-reactor creep of zirconium alloys are inter-dependent. Their effects on the creep of Zr–2.5Nb have been assessed using stress relaxation experiments [14]. Four pressure tube materials having different fabrication routes, described in ref. [15], were tested in four facilities in the NRU test reactor with various combinations of fast neutron fluxes and temperatures. Typical stress relaxation data for transverse specimens of one of the materials are shown in fig. 6, plotted as $\ln \sigma/\sigma_0$ against fluence. The stress ratio decreases linearly with fluence in all test conditions, in accordance with eq. (6). The

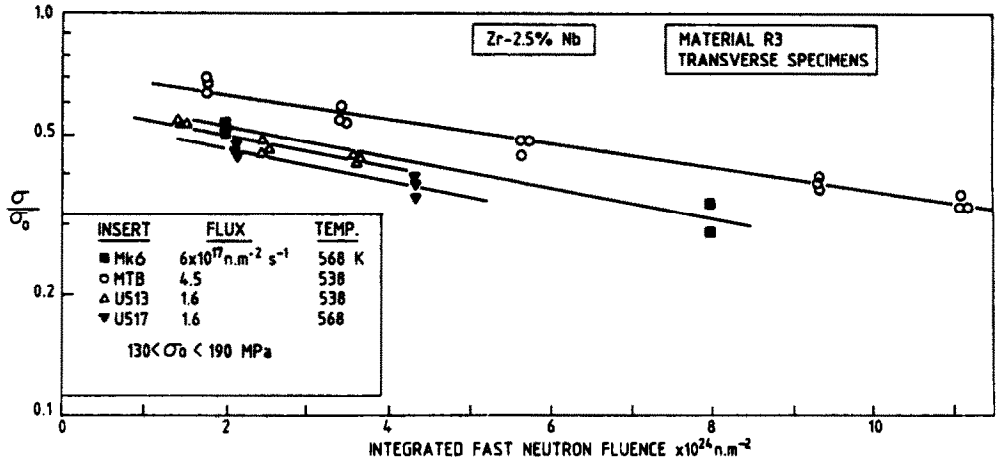

Fig. 6. Stress relaxation of transverse specimens of cold-worked Zr–2.5 Nb material R3 described in ref. [15] in four inserts with different temperature and fast neutron flux as a function of fluence.

relaxation rate constants are listed in table 1 for the four materials and test conditions. The data were fitted to the equation in which the creep rate, $\dot{\epsilon}_d$, is given by

$$\dot{\epsilon}_d = K_d/E_d\sigma = C_d K_c \phi^n \sigma \exp(-Q/T), \quad (8)$$

where K_d, E_d, and C_d are the rate constant, Young's modulus and anisotropy factor for a specimen taken from direction d in the tube, K_c is the material creep constant, which depends on dislocation density, ϕ is the fast neutron flux, n is the flux exponent, σ is stress, Q is the temperature constant and T is temperature. Although the best fit to the data gives a value for n of 0.82, it is not statistically different from the value of 1.0 observed in in-reactor creep experiments [13]. The values of K_c and Q were 1.3×10^{-21} and 3000 K for a flux exponent of 0.82 and 2.4×10^{-26} and 2200 K for an exponent of 1.0, respectively.

Derived creep constants from relaxation tests on

Table 1
Effect of temperature and fast neutron flux on stress relaxation rate constants of cold-worked Zr–2.5Nb pressure tube alloys. The table gives the stress relaxation rate constant, $K \times 10^{-4}$ $h^{-1} \pm 95\%$ CL [b]

Material [c]	Specimen orientation [d]	Test conditions [a]			
		A	B	C	D
R1	L	0.7±0.3	1.8±0.3	1.1±0.3	2.7±0.5
	T	0.5±0.2	1.1±0.2	0.8±0.4	2.5±0.7
R2	L	0.6±0.3	2.1±0.3	0.9±0.1	2.5±0.7
	T	0.5±0.1	1.0±0.3	0.7±0.2	1.6±0.3
R3	L	0.8±0.2	2.0±0.4	0.9±0.2	2.8±5.6
	T	0.5±0.1	1.1±0.2	0.6±0.2	1.8±1.3
Darlington [e]	L	0.7±0.2	1.6±0.4	1.0±0.1	3.2±0.8
	T	0.5±0.3	1.1±0.2	0.8±0.5	2.1±0.2

[a] Test conditions:
A: 538 K and 1.8×10^{17} n/m^2 s.
B: 568 K and 1.8×10^{17} n/m^2 s.
C: 538 K and 4.5×10^{17} n/m^2 s.
D: 573 K and 6.0×10^{17} n/m^2 s.

[b] 95% confidence limit.

[c] Pressure tubes materials are described in ref. [15].

[d] L = longitudinal, T = transverse directions in tube.

[e] Current CANDU production pressure tube.

Table 2
Creep constants derived from stress relaxation tests at 340 and 570 K, and their ratio [16]

Material	$C \times 10^{30}$ ((n/m^2)$^{-1}$ MPa^{-1})		Ratio C_{340}/C_{570}
	340 K	570 K	
Ni	2.4	1.8	1.33
Inconel X-750	1.3	0.5	2.6
304 SS	0.28	0.25	1.1
403 SS	0.27	0.20	1.4
410 SS	0.2	0.1	2.0
4140 steel	0.6	0.2	3.0
Zircaloy-2	0.4	0.4 [a)]	1.0
Zr–2.5Nb	2.3	2.7	0.85
Zr_3Al	1.0	0.8	1.25

[a)] This value was obtained after an initial stress decrease which lasted about 3000 h.

Zr–2.5 Nb and Zircaloy-2 at 570 and 320 K are listed in table 2, along with creep constants for several other metals and alloys which were tested in the same experiments [16]. The general trend of equal or higher creep rate at the lower temperature, which is observed for all metals in the table except Zr–2.5Nb, is consistent with results from other in-reactor stress relaxation and creep experiments carried out using different testing techniques [16].

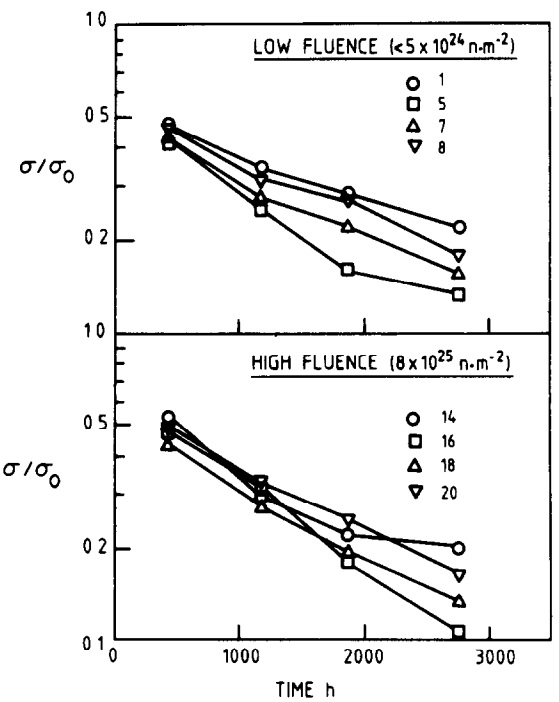

Fig. 7. Stress relaxation as a function of time for low- and high-fluence specimens from pre-irradiated annealed Zircaloy-4 guide tube after re-irradiation in Advanced Test Reactor [17].

The effect of fluence on the creep rate has been investigated by stress relaxation tests on pre-irradiated material. Fig. 7 shows results for annealed Zircaloy-4 specimens pre-irradiated to 8×10^{25} and 5×10^{24} n/m^2 as part of a fuel guide tube in a PWR [17]. Statistical analysis found that the relaxation rate increased by about 40% with the higher fluence. However, the relaxation tests were done at 330 K, whereas the guide tubes operated at about 553 K, thus, the relaxation test indicates that material with an irradiation-induced microstructure which results in accelerated irradiation growth at high fluences in annealed Zircaloy-2 at temperatures above 500 K [18], will also show an increase in creep rate at lower temperatures.

3.2. Alloy content

Several stress relaxation experiments on zirconium alloys have shown that the alloy content affects the creep behaviour in a manner which depends strongly on the thermo-mechanical treatment of the material [11,19]. The two zirconium alloys that have been utilized most extensively are binary alloys, with tin in Zircaloy and niobium in Zr–2.5Nb. Stress relaxation results from tests at about 570 and 330 K indicate that the tin in Zircaloy, which forms an α-phase solid solution hardener, has more creep strength than the niobium in Zr–2.5Nb, which forms a β-phase strengthener, at the lower temperature, while the converse holds at 570 K [19]. The effect of alloying elements iron and chromium, which are also β-phase stabilizers, on the relaxation constant at 570 K appears to be small compared with that of tin and niobium, as shown in table 3, partly because the heat treatment given the Zr–1.15 Cr–0.2Fe alloy resulted in almost complete precipitation of the chromium. Tin and aluminum do not decrease the relaxation constants in the alloys which have niobium and/or molybdenum additions, as shown in table 3. Stress relaxation results for a Zr_3Al alloy indicate that the intermetallic compound has a creep rate at 570 K comparable with those of the α-phase or β-phase zirconium alloys [20]. The creep strength of Excel alloy, a zirconium–tin–niobium–molybdenum alloy, which is being developed as a back-up to the Zr–2.5Nb pressure tube material in CANDU reactors, has been shown by stress relaxation tests to be better than than of the Zr–2.5Nb alloy, table 3 [21].

Table 3
Summary of relaxation rate constants of zirconium alloy pressure tubes tested at 570 K and 2×10^{17} n/m^2 s [20,21]

Material	Specimen orientation [a]	Relaxation rate constant (1×10^{-4} h^{-1})	Creep rate relative to CW Zr–2.5Nb
CW Zr–2.5Nb	L	1.6	1.0
	T	1.0	1.0
CW Zircaloy-2	L	1.8	1.1
	T	1.2	1.2
Zr–1.1Cr–0.2Fe [b]	L	1.9	1.2
Ann Excel [c]	L	0.6	0.4
	T	0.4	0.25
CW Excel	L	1.0	0.6
	T	0.7	0.45

[a] L = longitudinal, T-transverse directions in tube.
[b] Small tube material.
[c] Excel alloy composition Zr–3.5Sn–0.8Mo–0.8Nb.

Creep rates derived from stress relaxation tests on a series of binary zirconium alloys at 330 K, shown in table 4, indicate that a small amount of oxygen, iron, niobium, tin or gold suppressed the creep rate in both annealed and cold-worked alloys [22]. Increasing the tin content from 0 to 0.2 to 1.5 wt% results in progressive decreases in creep rate, while subsequent increases to 5 and 8 wt% show little further change. This pattern is also evident in the zirconium–niobium alloys, with little further increase after 0.6 wt%. Aging the zirconium–molybdenum alloys at different temperatures after quenching from the β-phase results in increased creep rate after the high-temperature aging. The effects of these alloying elements is related to their efficiency as trapping sites for the irradiation-induced interstitials and vacancies which affect the dislocation climb rates [22].

Table 4
Creep rates of binary zirconium alloys derived from stress relaxation tests at 320 K and 1.6×10^{17} n/m^2 s ($E>1$ MeV) [22]

Wt% solute content	Creep rate $\times10^{-10}$ (h^{-1} MPa^{-1})	
	Annealed material	CW material
Sponge Zr	1.0	2.0
0.2 O	0.2	0.8
0.2 Fe	0.3	0.9
0.15 Nb	0.3	0.6
0.6 Nb	0.4	
1.0 Nb	0.5	
20 Nb	0.4	
0.2 Sn	0.6	1.5
1.5 Sn	0.1	0.4
5 Sn	0.2	0.4
8 Sn	0.1 [a]	
1 Al	0.8	
3 Al	0.5	
2 Mo	0.3 [b]	0.4
2 Mo	0.5 [a]	
0.04 Au	0.1	1.4

[a] Quenched + aged at 873 K.
[b] Quenched + aged at 753 K.

3.3. Cold-work (dislocation density)

Increasing cold-work during the fabrication process results in an increase in the in-reactor creep rate of small Zr–2.5Nb tubes [23]. Results from stress relaxation tests, fig. 8, also show that cold-work is detrimental to the creep strength, with a greater effect on longitudinal specimens than on transverse specimens [13]. The dislocation density dependence of creep rates for cold-worked Zr–2.5Nb derived from creep measurements on power reactor and small tubes and helical springs, as well as stress relaxation tests, is shown in fig. 9 [24]. The creep data from the different stress modes are correlated by a model which assumes that the texture dependence of creep is related to the glide of dislocations on prism and pyramidal slip systems. The creep rate varies with dislocation density, as measured by X-ray diffraction, according to the relation $\dot{\epsilon} \propto \rho^p$, where p is 0.23 at 570 K. A similar correlation has been obtained for Zircaloy-2 stress relaxation data at 320 K, fig. 10, with p equal to 0.40 [25].

3.4. Anisotropy

The in-reactor creep behaviour of zirconium alloys is anisotropic, i.e. it depends on the testing direction in the sample [26]. Typical stress relaxation data from beam specimens cut from the longitudinal and transverse sections of a Zr–2.5Nb pressure tube are shown in fig. 11 [27]. The anisotropy is also evident in fig. 8, where the ratio of longitudinal to transverse relaxation rate remained constant independent of cold-work at about 1.8 [13]. Subsequent results found that the creep anisotropy ratios were 1.63 ± 0.25 and 1.30 ± 0.18 at 570 K, and 2.39 ± 0.25 and 1.49 ± 0.25 at 320 K, for Zr–2.5Nb and Zircaloy-2 tubes, respectively [27]. Thus, the anisotropy of creep in Zr–2.5Nb tubes is greater than that in Zircaloy-2 tubes, and is greater at 320 K than at 570 K for both alloys.

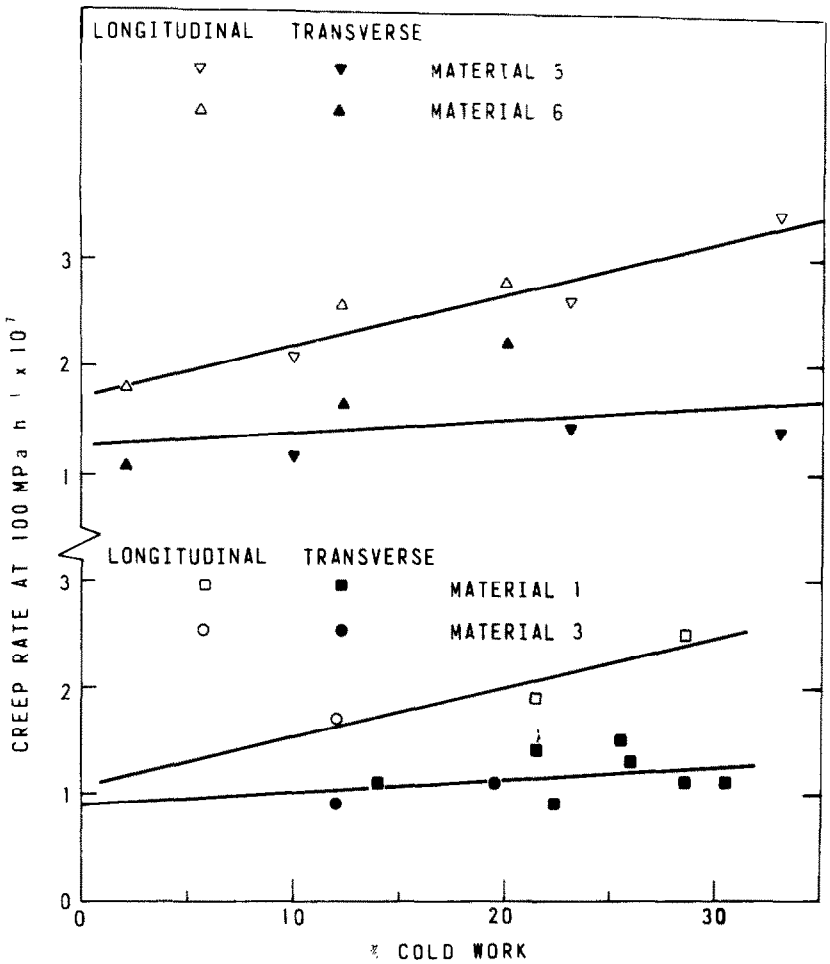

Fig. 8. Effect of cold-work after extrusion on creep rate of Zr–2.5Nb materials from stress relaxation tests in a fast neutron flux of 2×10^{17} n/m^2 s ($E>1$ MeV) at 570 K [13].

Holt and Ibrahim used creep anisotropy of Zr–2.5Nb materials derived from stress relaxation results to model the texture dependence of in-reactor creep of power reactor pressure tubes [26]. They postulated that the creep strain was due to slip of $\langle a \rangle$-types dislocation, primarily on prism planes, with secondary slip on basal planes. Subsequent analysis of the stress relaxation data, along with creep data from other stress modes, suggests that secondary slip on one of the pyramidal slip systems probably gives a better fit to the creep data [24].

3.5. Grain size

Kreyns and Burkart [9] found that the in-reactor creep rate of Zircaloy-2, derived from stress relaxation tests, increased by a factor of three as the grain size decreased by a factor of two. The results in fig. 12 [19], in which the relaxation rate constant is plotted as a function of an "operative grain size", based on the thickness of the α-phase grains, however, show that the effect of grain size on in-reactor creep of zirconium alloys is very small.

3.6. Strain recovery annealing

Strain recovery by post-irradiation annealing of stress relaxation [7–9], irradiation growth [28] and creep [29] specimens deformed in-reactor has been carried out by several workers with the aim of helping to identify the strain mechanisms. We have annealed unstressed irradi-

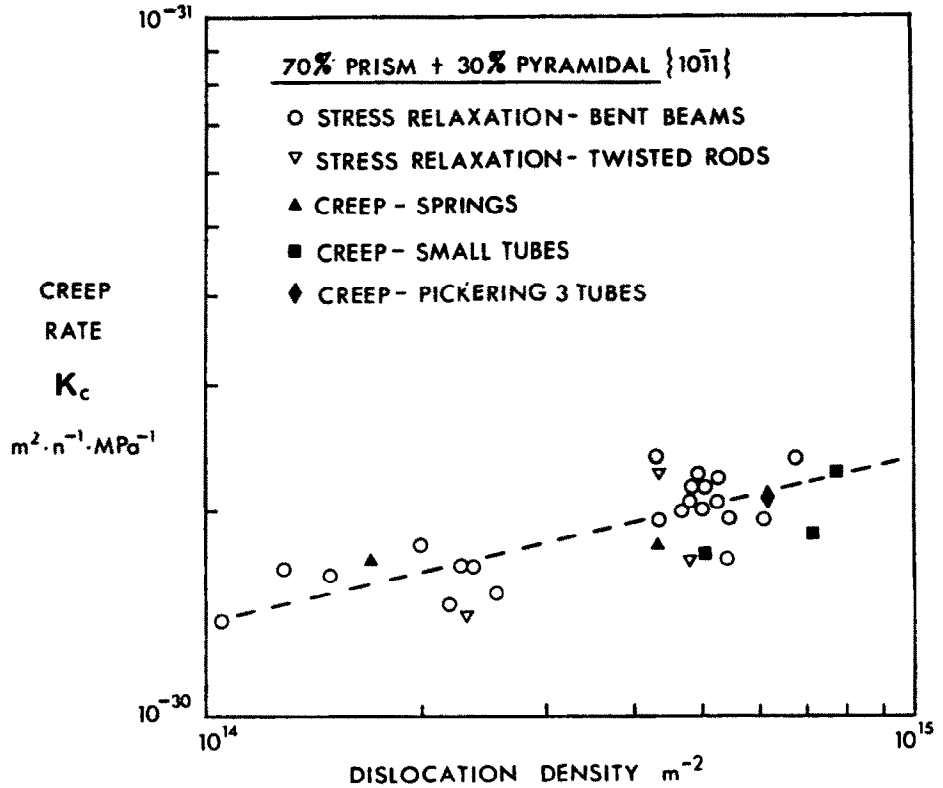

Fig. 9. In-reactor creep rate as a function of dislocation density for cold-worked Zr–2.5Nb using a creep model based on prism and pyramidal slip to correlate creep rates from different stress modes [24].

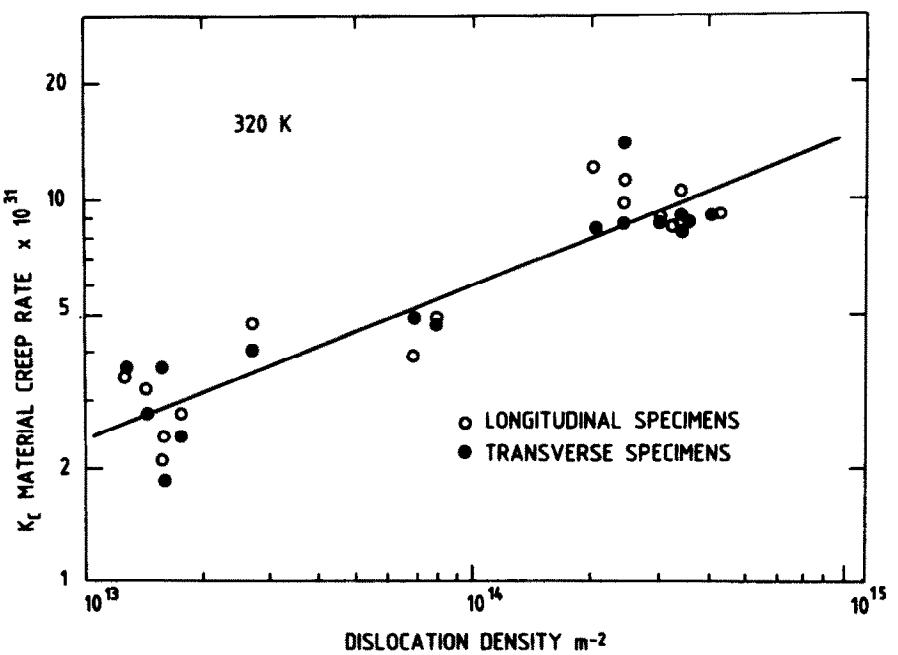

Fig. 10. In-reactor creep of Zircaloy-2 at 320 K, showing variation of material constant K_c with dislocation density [25].

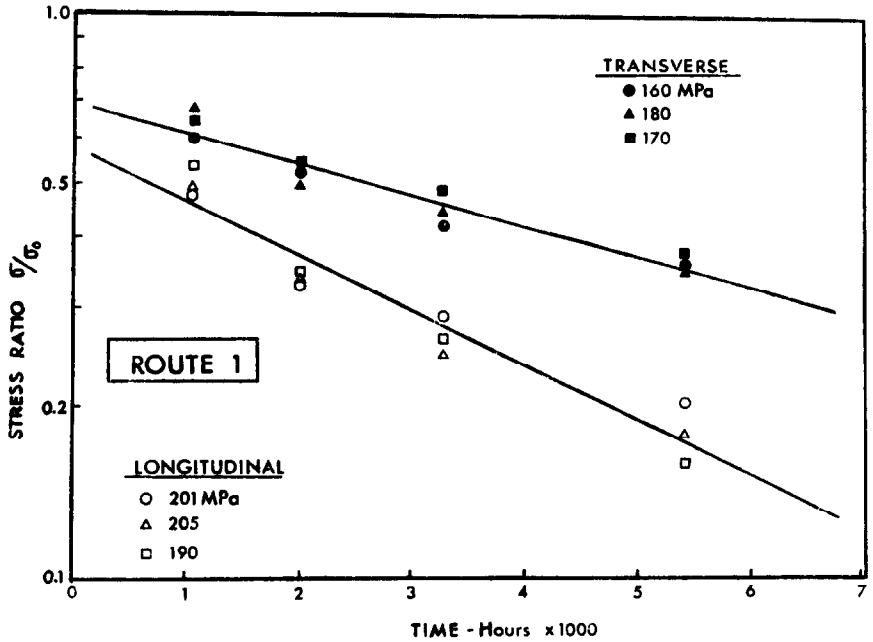

Fig. 11. Stress relaxation of Zr–2.5Nb pressure tube material at 570 K in a fast neutron flux of 2×10^{17} n/m^2 s ($E>1$ MeV), showing effect of orientation of test specimens on relaxation behaviour.

ated stress relaxation specimens out-reactor [30] and in the original in-reactor insert [31]. In general, although the amount of recovered strain is small, it amounts to a significant fraction of the original applied and stress relaxed strain.

Results from typical 1-hour isochronal anneals at temperatures from 570 to 770 K on Zircaloy-2 specimens [30], which were stress relaxed at 570 K with and without irradiation [10], are shown in fig. 13. The strain recovery continues with increasing temperature up to

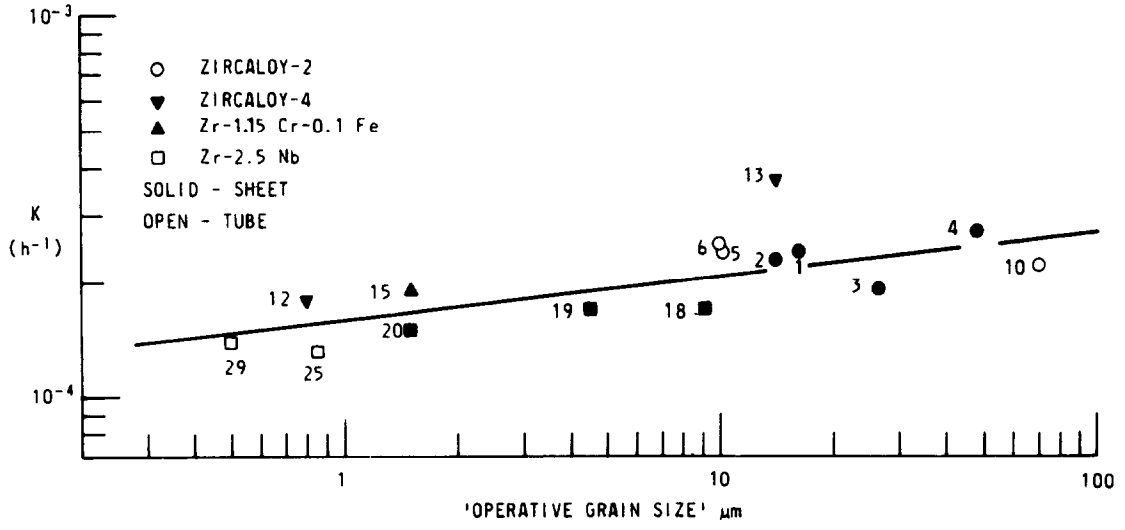

Fig. 12. Relaxation rate constant for longitudinal specimens as a function of "operative grain size" [19].

Table 5
Strain recovery for specimens stress relaxed for about 7000 h at 570 K (a) in an autoclave or (b) in-reactor, then annealed at 670 K for 300–500 h

Material	(a) Unirradiated			(b) Irradiated	
	Spec. orient. [a]	Relaxation strain (%)	Recovered strain (%)	Relaxation strain (%)	Recovered strain (%)
CW Zircaloy-2 [b]	L	0.145	0.035	0.194	0.037
	T	0.143	0.035	0.174	0.040
SR Zircaloy-2 [c]	L	0.075	0.037	0.176	0.077
	T	0.086	0.046	0.161	0.081
CW Zr–2.5Nb	L	0.158	0.031	0.198	0.037
	T	0.158	0.035	0.163	0.035
Q&A Zr–2.5Nb [d]	L	0.117	0.053	0.161	0.068
	T	0.079	0.057	0.108	0.066
Ann. Zircaloy-4 [e]	L	0.130	0.018	0.205	0.111
CW Zircaloy-2	L	0.163	0.037	0.213	0.035

[a] L = longitudinal, T = transverse directions in tube.
[b] Cold-worked tube.
[c] Cold-worked and stress-relieved tube.
[d] Quenched, cold-worked and aged tube.
[e] Annealed sheet.

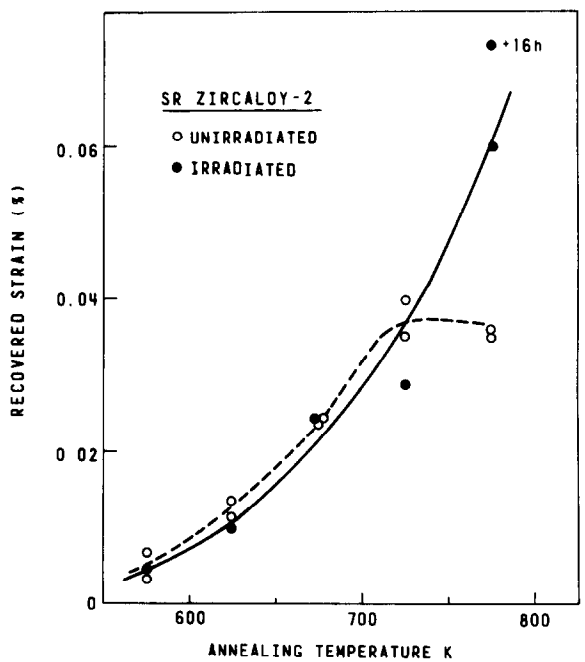

Fig. 13. Recovered strain from consecutive 1 h isochronal anneals in stress-relieved Zircaloy-2 specimens [30].

770 K in irradiated specimens, but stops above 720 K in unirradiated specimens. The strain recovery behaviour during isothermal annealing at 670 K, shown in fig. 14, suggests that the rapid initial recovery observed in irradiated and unirradiated specimens is anelastic in nature, perhaps attributable to unbowing of bowed-out dislocations. Subsequent recovery in irradiated specimens may also be considered to be anelastic, since irradiation-enhanced dislocation climb would have contributed to further dislocation bow-out, but could also be due to annealing of irradiation damage [32]. However, since dislocation glide enabled by enhanced dislocation climb is also a probable in-reactor creep mechanism, the anelastic nature of in-reactor stress relaxation does not preclude its useful contribution to the understanding of in-reactor creep behaviour. In table 5 the recovered strains for different zirconium alloys indicate that the metallurgical condition of the specimen affects the amount of recovered strain [30]. A smaller fraction of the relaxed strain is recovered in cold-worked specimens than in annealed or stress relieved specimens.

The results from an experiment [31] in which stress relaxation specimens were reirradiated unstressed are shown in table 6. All recovered strains are similar

Table 6
Strain recovery for specimens stress relaxed in-reactor, then reirradiated unstressed for 4500 h [31]

Temperature (K)	Material	Relaxed time (h)	Applied strain (%)	Relaxed strain (%)	Recovered strain (%)
545	Excel [a]	14400	0.32	0.21	0.04
	Zr–2.5Nb	9800	0.20	0.12	0.03
	Zr–2.5Nb	14400	0.28	0.21	0.04
573	Excel	14400	0.36	0.14	0.04
	Excel	3900	0.40	0.10	0.05
	Zr–2.5Nb	14400	0.40	0.30	0.05
	Zr–2.5Nb	3900	0.38	0.17	0.07

[a] Excel alloy composition Zr–3.5Sn–0.8Mo–0.8Nb.

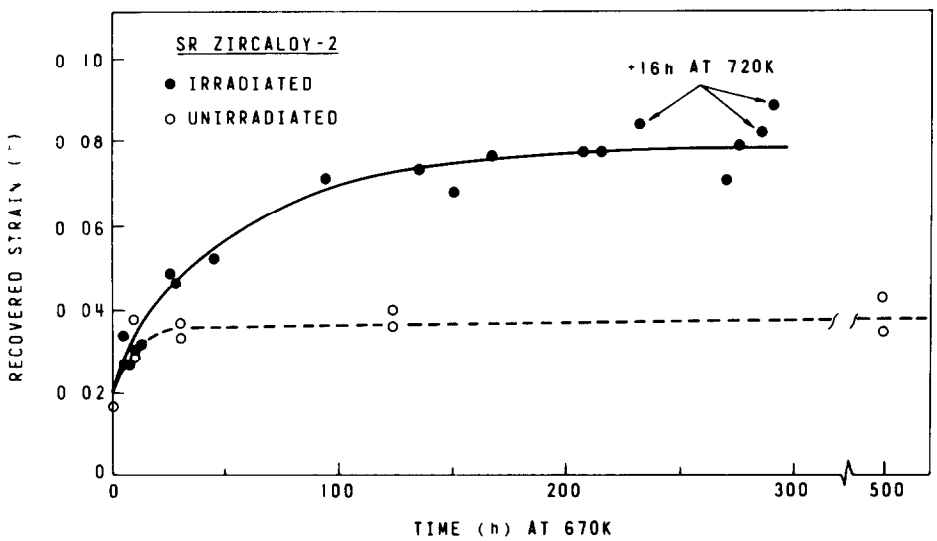

Fig. 14. Recovered strain from isothermal annealing at 670 K in stress-relieved Zircaloy-2 specimens [30].

regardless of the relaxation times. The fact that all strain in specimens which were only relaxed 4000 h is not recovered after 4500 h re-irradiation, also supports the idea that stress relaxation strain is due to creep-related mechanisms.

4. Summary

In-reactor stress relaxation tests have been shown to be a simple, robust, versatile and relatively inexpensive experimental technique for the evaluation of the in-reactor creep behaviour of zirconium alloys. The tests have some experimental limitations in that the strain is restricted to one elastic deflection and there is an attendant decrease in accuracy with test time as the stress drops. Assumptions must be made in translating relaxation results into creep data which necessitate establishing experimental correlations. The independence of the stress ratio on the initial stress and the linear decrease in $\ln \sigma/\sigma_0$ with time support the use of the in-reactor creep law in eq.(4) and the derived stress relaxation expression in eq. (6). The experimental correlations shown in figs. 4 and 5 strongly indicate that the stress relaxation behaviour is related to the creep behaviour.

The results on the effects of temperature and flux on in-reactor stress relaxation are consistent with results from other creep testing modes where comparisons can be made, while the measured effect of fluence is an excellent example of how the stress relaxation test can supplement creep testing by providing "snapshot" looks at pre-irradiated materials. The tests which showed an

increase in creep rate with fluence indicate that creep rates are strongly dependent on the microstructure developed during irradiation, which in turn is dependent on temperature. The increase in creep rate observed would not be expected to affect reactor components, such as CANDU reactor calandria tubes, which operate only at temperatures around 330 K because the necessary microstructure probably will not develop during reactor lifetime fluences.

Stress relaxation tests on different alloys and thermo-mechanical treatments indicate that the creep strength of zirconium alloys can be enhanced by controlling the microstructural parameters. Particularly noteworthy is the contribution of stress relaxation testing to the study of the effect of crystallographic texture on irradiation-enhanced creep. The stress relaxation anisotropy ratios have made a significant contribution to the development of models to account for the effect of texture [24,26]. The recently proposed model by Woo [33,34], based on the self-consistent calculation for intergranular constraints, required creep data from at least three independent stress modes, which are only available from stress relaxation tests on longitudinal and transverse bent beams and torsion rods [24]. The deleterious effect of cold-work observed in other creep tests has been extended and quantified by correlations with dislocation density [24,25].

From an applications point of view, bent-beam stress relaxation tests on longitudinal strips from pressure tubes and calandria tubes give bending creep data which are most relevant for estimating sag of CANDU fuel channels. In fact, because the calandria tubes in CANDU reactors are inaccessible for measurement under normal operation, strain rates derived from stress relaxation tests have provided the only means of estimating the in-reactor creep rates of these reactor components. Good agreement was found between fuel channel sag behaviour calculated using these strain rates and that measured during monitoring inspections [35].

References

[1] V. Fidleris, The Zircaloy-2 In-Pile Creep Measurements at Chalk River, ASME Winter Annual Meeting (1962) paper 62-WA-325.

[2] P.A. Ross-Ross and C.E.L. Hunt, J. Nucl. Mater. 26 (1968) 2.

[3] W.K. Alexander, V. Fidleris and R.A. Holt, ASTM STP 633 (1976) 344.

[4] A.R. Causey, S.R. MacEwen, H.C. Jamieson and A.B. Mitchell, Res. Mech. 2 (1981) 211.

[5] R.L. Mehan, Trans. ASME 226 (1959).

[6] J.W. Joseph, Jr., Savannah River (USA) Report DP-623 (1961).

[7] P.A. Platonov, IAEA, USAEC Report AEC-TR-5257 (1962).

[8] R.V. Hesketh, Philos. Mag. 8 (1963) 1321.

[9] P.H. Kreyns and M.W, Burkart, J. Nucl. Mater. 26 (1968) 87.

[10] D.E. Fraser, P.A. Ross-Ross and A.R. Causey, J. Nucl. Mater. 46 (1973) 281.

[11] A.R. Causey, J. Nucl. Mater. 54 (1974) 64.

[12] V. Fidleris, J. Nucl. Mater. 26 (1968) 51.

[13] C.E. Coleman, A.R. Causey and V. Fidleris, AECL Report AECL-5042 (1975).

[14] F.J. Butcher and S.A. Dononue, unpublished results.

[15] J.D. Parker, V. Perovic, M. Leger and R.G. Fleck, ASTM STP 939 (1987) 86.

[16] A.R. Causey, S.R. MacEwen and G.J.C. Carpenter, J. Nucl. Mater., 90 (1980) 216.

[17] A.R. Causey, V. Fidleris and R.A. Holt, J. Nucl. Mater. 139 (1986) 277.

[18] R.A. Holt and R.W. Gilbert, J. Nucl. Mater. 137 (1986) 185.

[19] A.R. Causey, ATSM STP 551 (1974) 263.

[20] A.R. Causey, V. Fidleris, H.E. Rosinger, E.M. Schulson and V.F. Urbanic, ASTM STP 633 (1977) 437.

[21] B.A. Cheadle, R.A. Holt, V. Fidleris, A.R. Causey and V.F. Urbanic, ASTM STP 754 (1982) 193.

[22] A.R. Causey and R.H. Zee, unpublished results.

[23] E.F. Ibrahim, J. Nucl. Mater. 118 (1983) 260.

[24] A.R. Causey, R.A. Holt and S.R. MacEwen, ASTM STP 824 (1984) 269.

[25] V. Fidleris, A.R. Causey and R.A. Holt, Optimising Materials for Nuclear Applications, Eds. F.A. Garner, D.S. Gelles and F.W. Wiffen (TMS, 1984) p. 35.

[26] R.A. Holt and E.F. Ibrahim, Acta Metall. 27 (1979) 1319.

[27] A.R. Causey, J. Nucl. Mater. 98 (1981) 313.

[28] R.B. Adamson, in: Proc. BNES Conf., London, Nov. 1972, p. 305.

[29] G.R. Piercy and J. Lori, AECL Report AECL-3226 (1968).

[30] A.R. Causey, J. Nucl. Mater. 61 (1976) 71.

[31] S.A. Donohue and A.R. Causey, to be published.

[32] D.O. Northwood and A.R. Causey, J. Nucl. Mater. 64 (1977) 308.

[33] C.H. Woo, J. Nucl. Mater. 131 (1985) 105.

[34] C.H. Woo, Effects of intergranular interaction on the anisotropy of irradiation creep and growth in zirconium, in: Proc. Int. Conf. on Materials for Nuclear Reactor Core Applications (BNES, London, 1987).

[35] A.R. Causey, A.G. Norsworthy and C.W. Schulte, Can. Metall. Quart. 24 (1985) 207.